

A Unified Perspective on Natural Gradient Variational Inference with Gaussian Mixture Models

Oleg Arenz

*Intelligent Autonomous Systems
Technical University of Darmstadt*

oleg.arenz@tu-darmstadt.de

Philipp Dahlinger

*Autonomous Learning Robots
Karlsruhe Institute of Technology*

philipp.dahlinger@kit.edu

Zihan Ye

*Artificial Intelligence & Machine learning group
Hessian Center for AI (hessian.AI)
Technical University of Darmstadt*

zihan.ye@tu-darmstadt.de

Michael Volpp

Gerhard Neumann
*Autonomous Learning Robots
Karlsruhe Institute of Technology*

*michael.volpp@kit.edu
gerhard.neumann@kit.edu*

Abstract

Variational inference with Gaussian mixture models (GMMs) enables learning of highly-tractable yet multi-modal approximations of intractable target distributions. GMMs are particularly relevant for problem settings with up to a few hundred dimensions, for example in robotics, for modelling distributions over trajectories or joint distributions. This work focuses on two very effective methods for GMM-based variational inference that both employ independent natural gradient updates for the individual components and the categorical distribution of the weights. We show for the first time, that their derived updates are equivalent, although their practical implementations and theoretical guarantees differ. We identify several design choices that distinguish both approaches, namely with respect to sample selection, natural gradient estimation, stepsize adaptation, and whether trust regions are enforced or the number of components adapted. We perform extensive ablations on these design choices and show that they strongly affect the efficiency of the optimization and the variability of the learned distribution. Based on our insights, we propose a novel instantiation of our generalized framework, that combines first-order natural gradient estimates with trust-regions and component adaption, and significantly outperforms both previous methods in all our experiments.

1 Introduction

Many problems in machine learning involve inference from intractable distributions $p(\mathbf{x})$, that might further only be known up to a normalizing constant Z , that is,

$$p(\mathbf{x}) = \frac{1}{Z} \tilde{p}(\mathbf{x}).$$

For example, in Bayesian inference, the intractable, unnormalized target distribution $\tilde{p}(\mathbf{x})$ corresponds to the product of prior and likelihood and the normalizing constant can not be computed in closed form. Variational inference (VI) aims to approximate the intractable target distribution $\tilde{p}(\mathbf{x})$ by means of a tractable, parametric model $\tilde{q}_{\boldsymbol{\theta}}(\mathbf{x})$, with parameters $\boldsymbol{\theta}$, which can then be used for inference.

Gaussian mixture models are a simple yet powerful choice for a model family, since they can approximate arbitrary distributions, when assuming a sufficiently high number of components. Compared to more complex models, such as normalizing flows (Kobyzev et al., 2020), they are more interpretable and tractable since not only sampling and evaluating GMMs is cheap, but also marginalizations and certain expectations (of linear or quadratic functions) can be computed in closed form. Furthermore, the simplicity of GMMs allows for sample-efficient learning algorithms, that is, algorithms that require relatively few evaluations of the unnormalized target distribution for learning the model parameters θ (which correspond to the weights, means and covariance matrices of the GMM). GMM-based variational inference is in particular relevant for problem settings with up to a few hundred dimensions, where learning and storing of full covariance matrices is still tractable. Such problems occur, for example, in robotics, where GMM-based VI has been successfully applied for modeling multimodal distributions over trajectories (Ewerton et al., 2020) and joint configurations (Pignat et al., 2020).

Arguably the two most effective algorithms for GMM-based variational inference, both apply independent natural gradient updates on each component as well as on the categorical distribution over weights (Arenz et al., 2018; Lin et al., 2019a). Yet, both algorithms were derived from a different perspective, have different theoretical guarantees, and even different objectives for the independent updates. Namely, Lin et al. (2019a; 2020) use the original GMM objective for each independent update and show that this procedure performs natural gradient descent also with respect to the full mixture model, whereas VIPS (Arenz et al., 2018; 2020) uses a lower bound for an expectation-maximization procedure, which yields independent objective functions for each component and the mixture weights. Their approach can be shown to converge, even when the M-Step does not consist of single natural gradient updates, however, it was not yet proven, that their proposed procedure, which does use single natural gradient steps, also performs natural gradient descent on the full mixture.

In this work, we show that the proposed updates of both procedures are in fact the same because, directly after the E-Step, the (natural) gradients of the lower bound objectives of VIPS momentarily match the gradients of the original objective. However, despite the theoretical equivalence of both updates, their reference implementations perform very differently due to several design choices, as we will show in our experiments. Namely, VIPS use samples from the individual component to estimate the natural gradient using the policy search method MORE (Abdolmaleki et al., 2015), which is also applicable to non-differentiable target distribution, whereas Lin et al. (2020) sample from the GMM and use Stein’s Lemma (Lin et al., 2019b), which makes use of gradients and is, thus, less general, but more efficient. Furthermore, Lin et al. (2020) directly control the learning rates, whereas Arenz et al. (2018) use adaptive trust-regions based on the Kullback-Leibler divergence (Kullback and Leibler, 1951), and Lin et al. (2020) fix the number of components a priori, whereas Arenz et al. (2018) proposed to adapt them during optimization. We perform extensive ablations to evaluate the effects of these design choices in terms of sample efficiency, training stability and exploration, and show that a hybrid approach outperforms both previous methods significantly. We summarize our main contributions as follows:

- We improve our theoretical understanding of GMM-based variational inference by connecting the two previously separated lines of research by Arenz et al. (2018; 2020) and Lin et al. (2019a; 2020). Our results imply that VIPS performs natural gradient descent on the whole GMM.
- We evaluate the effects of several design choices and propose a novel method that significantly outperforms both previous methods. In particular, our proposed method combines KL-constrained trust regions, which have been popularized in the gradient-free reinforcement learning setting (Peters et al., 2010; Schulman et al., 2015; Otto et al., 2021), with gradient-based estimates of the natural gradient (Lin et al., 2019b).

2 Natural Gradient Updates for GMMs

We will now review the typical optimization problem for variational inference, and prior works that are central to our contributions, namely VIPS (Arenz et al., 2018; 2020) and a line of research for higher natural gradient estimates for VI (Lin et al., 2019b;a; 2020).

2.1 Problem Formulation

The problem of approximating a target distribution $p(\mathbf{x})$ with a model $q_{\boldsymbol{\theta}}(\mathbf{x})$ is typically framed as the problem of minimizing the reverse Kullback-Leibler divergence (Kullback and Leibler, 1951), $\text{KL}(q_{\boldsymbol{\theta}}||p)$, which is defined as

$$\begin{aligned}\text{KL}(q_{\boldsymbol{\theta}}||p) &= \int_{\mathbf{x}} q_{\boldsymbol{\theta}}(\mathbf{x}) \log \frac{q_{\boldsymbol{\theta}}(\mathbf{x})}{p(\mathbf{x})} d\mathbf{x} \\ &= \int_{\mathbf{x}} q_{\boldsymbol{\theta}}(\mathbf{x}) \log \frac{q_{\boldsymbol{\theta}}(\mathbf{x})}{\tilde{p}(\mathbf{x})} d\mathbf{x} + \log Z.\end{aligned}$$

The reverse Kullback-Leibler divergence is a principled choice for the optimization problem, as it directly corresponds to the average amount of information (measured in nats), that samples from the approximation $q_{\boldsymbol{\theta}}(\mathbf{x})$ contain for discriminating between the approximation and the target distribution. Furthermore, the optimization can be performed despite the intractability of the normalizing constant, which is a constant offset to the objective function and, thus, does not affect the optimal parameters $\boldsymbol{\theta}$. When ignoring the normalizing constant and reframing the minimization problem as a maximization problem, we obtain the evidence lower bound objective (ELBO). When the variational distribution $q_{\boldsymbol{\theta}}(\mathbf{x})$ corresponds to a Gaussian mixture model $q_{\boldsymbol{\theta}}(\mathbf{x}) = \sum_o q_{\boldsymbol{\theta}}(o)q_{\boldsymbol{\theta}}(\mathbf{x}|o)$, with weights $q_{\boldsymbol{\theta}}(o)$ and Gaussian components $q_{\boldsymbol{\theta}}(\mathbf{x}|o)$, the ELBO is given by

$$J(\boldsymbol{\theta}) = \sum_o q_{\boldsymbol{\theta}}(o) \int_{\mathbf{x}} q_{\boldsymbol{\theta}}(\mathbf{x}|o) \log \tilde{p}(\mathbf{x}) d\mathbf{x} + H(q_{\boldsymbol{\theta}}), \quad (1)$$

where

$$H(q_{\boldsymbol{\theta}}) = - \int_{\mathbf{x}} q_{\boldsymbol{\theta}}(\mathbf{x}) \log(q_{\boldsymbol{\theta}}(\mathbf{x})) d\mathbf{x}$$

denotes the entropy of the GMM. Hence, our objective is to maximize Equation 1 with respect to the parameters $\boldsymbol{\theta}$, that correspond to the weights $q(o)$ and the mean and covariance matrix for each Gaussian component $q(\mathbf{x}|o)$. Different methods have been proposed to (i) decompose the NG update for the whole GMM into an individual NG update for each component and (ii) how to update each component using either zero-order or first-order information and (iii) how to update the weights of the GMM.

2.2 Updating the Components

In this section, we will focus our discussion on updating a single Gaussian component $h(\mathbf{x}) = q(\mathbf{x}|o)$ with mean $\boldsymbol{\mu}$ and variance $\boldsymbol{\Sigma}$ with respect to an auxiliary ELBO,

$$\begin{aligned}\tilde{J}_h &= \int_{\mathbf{x}} h(\mathbf{x}) R(\mathbf{x}) d\mathbf{x} + H(h(\mathbf{x})) \\ &= \mathbb{E}_{h(\mathbf{x})} [f(\mathbf{x})] \text{ with } f(\mathbf{x}) = R(\mathbf{x}) - \log h(\mathbf{x}).\end{aligned} \quad (2)$$

How this auxiliary ELBO is obtained from the full GMM objective and how $R(\mathbf{x})$ is defined is discussed in Section 2.3.1.

2.2.1 Zero-order NG Updates

Arenz et al. (2018) use the policy search method MORE (Abdolmaleki et al., 2015), which first learns a quadratic approximation $\tilde{R}(\mathbf{x}) \approx R(\mathbf{x})$ using ordinary least-squares based on sample evaluations of $\tilde{p}(\mathbf{x})$ and then solves the surrogate objective, subject to a trust-region constraint, that ensures that the KL divergence between the updated distribution and the last distribution $h_{\text{old}}(\mathbf{x})$ is smaller than a given bound ϵ (a hyperparameter similar to a learning rate),

$$\begin{aligned}\arg \max_{h(\mathbf{x})} & \int_{\mathbf{x}} h(\mathbf{x}) \tilde{R}(\mathbf{x}) d\mathbf{x} + H(h(\mathbf{x})), \\ \text{s.t.} & \quad \text{KL}(h(\mathbf{x})||h_{\text{old}}(\mathbf{x})) \leq \epsilon.\end{aligned} \quad (3)$$

For a quadratic surrogate

$$\tilde{R}(\mathbf{x}) = \frac{1}{2} \mathbf{x}^\top \mathbf{R} \mathbf{x} + \mathbf{x}^\top \mathbf{r} + r,$$

where the matrix \mathbf{R} , the vector \mathbf{r} and the scalar r are learned using least-squares, the optimal mean and covariance for optimization problem 3 are given by

$$\begin{aligned} \Sigma &= \left(\frac{\eta}{\eta+1} \Sigma_{\text{old}}^{-1} - \frac{1}{\eta+1} \mathbf{R} \right)^{-1}, \\ \mu &= \Sigma \left(\frac{\eta}{\eta+1} \Sigma_{\text{old}}^{-1} \mu_{\text{old}} + \frac{1}{\eta+1} \mathbf{r} \right), \end{aligned} \quad (4)$$

where η is the Lagrangian multiplier for the trust region constraint that can be efficiently found by minimizing the Lagrangian dual objective (Abdolmaleki et al., 2015). The updates based on Equation 4 are along the natural gradient because the quadratic surrogate is a compatible function approximator for Gaussian distributions (Pajarinen et al., 2019; Sutton et al., 2000). Due to the use of ordinary least-squares to obtain the NG, the MORE update only uses function evaluations and no gradient information of $R(\mathbf{x})$. However, the gradient of the target distribution, that acts as the reward function in this formulation, is typically available in VI and could be exploited to significantly increase sample efficiency (Lin et al., 2019b).

2.2.2 Higher-Order NG Updates

Khan and Nielsen (2018) show that for exponential-family distributions, the natural gradient with respect to the natural parameters λ (for Gaussians $\lambda = \{0.5\Sigma^{-1}, \Sigma^{-1}\mu\}$) corresponds to the vanilla gradient with respect to the expectation parameters \mathbf{m} (for Gaussians $\mathbf{m} = \{\Sigma + \mu\mu^\top, \mu\}$). Using the chain rule, the gradient with respect to the expectation parameters can be expressed in terms of the gradient with respect to the covariance Σ and mean μ (Khan and Lin, 2017, Appendix B.1). Combining these results, a natural gradient step for a Gaussian distribution $h(\mathbf{x}) = \mathcal{N}(\mathbf{x}; \mu, \Sigma)$ with stepsize β and objective J_h can be computed as

$$\Sigma = (\Sigma_{\text{old}}^{-1} - 2\beta \nabla_{\Sigma_o} J_h)^{-1}, \quad \mu = \mu_{\text{old}} + \beta \Sigma \nabla_{\mu} J_h, \quad (5)$$

as shown by Khan et al. (2018, Appendix C). As the objective J_h corresponds to an expected value, i.e., $J_h = \mathbb{E}_{h(\mathbf{x})}[f(\mathbf{x})]$ with $f(\mathbf{x}) = R(\mathbf{x}) - \log h(\mathbf{x})$, the gradient with respect to mean and covariance are given by the expected gradient and Hessian (Opper and Archambeau, 2009),

$$\nabla_{\Sigma} J_h = \frac{1}{2} \mathbb{E}_{h(\mathbf{x})} [\nabla_{\mathbf{x}\mathbf{x}} f(\mathbf{x})], \quad \nabla_{\mu} J_h = \mathbb{E}_{h(\mathbf{x})} [\nabla_{\mathbf{x}} f(\mathbf{x})]. \quad (6)$$

Hence, using Monte-Carlo to estimate the gradients with respect to mean and covariance (Eq. 6), we can obtain unbiased estimates of the natural gradient (Eq. 5). Further exploiting that the expected gradient and the expected Hessian of the log probability density of a Gaussian distribution are given by $\mathbb{E}_{h(\mathbf{x})}[\nabla_{\mathbf{x}\mathbf{x}} \log h(\mathbf{x})] = -\Sigma^{-1}$, and $\mathbb{E}_{h(\mathbf{x})}[\nabla_{\mathbf{x}} \log h(\mathbf{x})] = \mathbf{0}$, the natural gradient updates can be expressed in terms of gradients and Hessians of the target distribution

$$\begin{aligned} \Sigma &= ((1 - \beta) \Sigma_{\text{old}}^{-1} - \beta \mathbb{E}_{h(\mathbf{x})} [\nabla_{\mathbf{x}\mathbf{x}} R(\mathbf{x})])^{-1} \\ \mu &= \Sigma \left((1 - \beta) \Sigma_{\text{old}}^{-1} \mu_{\text{old}} - \beta \mathbb{E}_{h(\mathbf{x})} [\nabla_{\mathbf{x}} \log \tilde{p}(\mathbf{x})] \right. \\ &\quad \left. - \beta \mathbb{E}_{h(\mathbf{x})} [\nabla_{\mathbf{x}\mathbf{x}} \log R(\mathbf{x})] \mu_{\text{old}} \right). \end{aligned} \quad (7)$$

Khan and Lin (2017); Khan et al. (2018) proposed the second-order method VON, which directly uses a single sample Monte-Carlo estimate of Equation 7. More recently, Lin et al. (2019b) proposed an unbiased first order estimate of the expected Hessian by generalizing Stein's Lemma (Stein, 1981). Namely, as they show in Lemma 11, the expected Hessian is given by

$$\mathbb{E}_{h(\mathbf{x})} [\nabla_{\mathbf{x}\mathbf{x}} f(\mathbf{x})] = \mathbb{E}_{h(\mathbf{x})} [\Sigma^{-1} (\mathbf{x} - \mu) (\nabla_{\mathbf{x}} f(\mathbf{x}))^\top],$$

and, hence, can be estimated based on first-order information. Lin et al. (2020) further proposed a slight modification of the update in Eq. 7, which ensures that the new covariance matrix remains positive definite.

Yet, while the NG can now be computed from first-order information $\nabla_{\mathbf{x}} f(\mathbf{x})$, in contrast to zero-order methods, these algorithms do not exploit any probabilistic trust region. Consequently, the learning rate β needs to be set with care, disallowing the algorithm to make more aggressive updates in particular if the NG estimates are still noisy.

2.3 Obtaining Decomposed Updates per Component

Computing the NG for GMMs directly is difficult. However, estimating the NG for GMMs can be reduced to individual NG updates per component. This reduction has also been derived from different perspectives Arenz et al. (2018); Lin et al. (2019a).

2.3.1 Lower-bound Decomposition of the ELBO

Although the first term of the ELBO given in Equation 1 decomposes into independent objectives for each component, the second term (the model entropy) prevents us from optimizing each component independently. More specifically, when using Bayes theorem to write the probability density of the GMM in terms of the marginals and conditionals, the interdependence between the different components can be narrowed down to the (log-)responsibilities $q_{\theta}(o|\mathbf{x})$ within the entropy,

$$H(q_{\theta}) = - \sum_o q_{\theta}(o) \int_{\mathbf{x}} q_{\theta}(\mathbf{x}|o) \left(\log \frac{q_{\theta}(o)q_{\theta}(\mathbf{x}|o)}{q_{\theta}(o|\mathbf{x})} \right),$$

which is the only term in Equation 1 that creates a mutual dependence between different components. Hence, VIPS (Arenz et al., 2018) introduced an auxiliary distribution $\tilde{q}(o|\mathbf{x})$, to derive a lower bound $\tilde{J}(\tilde{q}, \theta)$ of Equation 1, that is given by

$$\begin{aligned} \tilde{J}(\tilde{q}, \theta) &= \sum_o q(o) \left[\int_{\mathbf{x}} q_{\theta}(\mathbf{x}|o) \left(\log \tilde{p}(\mathbf{x}) + \log \tilde{q}(o|\mathbf{x}) \right) d\mathbf{x} \right. \\ &\quad \left. + H(q_{\theta}(\mathbf{x}|o)) \right] + H(q_{\theta}(o)) \\ &= J(\theta) - \int_{\mathbf{x}} q_{\theta}(\mathbf{x}) \text{KL}(q(o|\mathbf{x}) || \tilde{q}(o|\mathbf{x})) d\mathbf{x}. \end{aligned} \tag{8}$$

As an expected KL is non-negative for any two distributions and equals zero, if both distributions are equal, $\tilde{J}(\tilde{q}, \theta)$ is a lower bound of $J(\theta)$, that is tight when $\tilde{q}(o|\mathbf{x}) = q(o|\mathbf{x})$. Hence, Arenz et al. (2018) proposed a procedure similar to expectation maximization that alternates between recomputing the responsibilities based on the current model parameters (E-Step), and optimizing the model parameters with respect to the lower bound $\tilde{J}(\tilde{q}, \theta)$. As the lower bound is tight, i.e, it matches the actual objective $J(\theta)$ before each M-step, the M-step always improves the original objective. As the auxiliary distribution $\tilde{q}(o|\mathbf{x})$ is independent of the model parameters (during the M-step), the optimization of the lower bound can be performed independently for the weights $q(o)$ and each component $q(\mathbf{x}|o)$, resulting in a component-wise loss function

$$\begin{aligned} \tilde{J}_o(\tilde{q}, \theta) &= \int_{\mathbf{x}} q_{\theta}(\mathbf{x}|o) \left(\log \tilde{p}(\mathbf{x}) + \log \tilde{q}(o|\mathbf{x}) \right. \\ &\quad \left. - \log q(\mathbf{x}|o) \right) d\mathbf{x}. \end{aligned} \tag{9}$$

Instead of Objective 2, this objective is now used to optimize the individual components. Relating Eq. 9 to the introduced objective in Eq. 2 for updating the single components, we can see that $R_o(\mathbf{x}) = \log \tilde{p}(\mathbf{x}) + \log \tilde{q}(o|\mathbf{x})$.

2.3.2 Fisher Information Matrix Decomposition

Whereas the aforementioned higher-order estimates of the natural gradient assume Gaussian variational approximations, Lin et al. (2019a) proposed natural gradient updates for more expressive model classes,

including Gaussian mixture models. Similar to VIPS, they show that the update can be decomposed into independent natural gradient updates for each component by realizing that the Fisher information matrix of the joint distribution $q_{\theta}(\mathbf{x}, o)$ (instead of the marginal $q_{\theta}(\mathbf{x})$) is well-defined. This allows for higher-order per-component natural gradient updates, although with a slight modified objective (Lin et al., 2019a),

$$\begin{aligned}\tilde{J}_{q(\mathbf{x}|o)} &= \int_{\mathbf{x}} q(\mathbf{x}|o) \log \frac{\tilde{p}(\mathbf{x})}{q(\mathbf{x})} d\mathbf{x} \\ &= \mathbb{E}_{q(\mathbf{x}|o)} [f(\mathbf{x})] \text{ with } f(\mathbf{x}) = \log \tilde{p}(\mathbf{x}) - \log q(\mathbf{x}).\end{aligned}\tag{10}$$

As we will show in Section 3, directly after performing the E-step, this objective momentarily aligns with Eq. 9.

2.4 Updating the Mixture Weights

Both algorithmic families also slightly differ in their updates of the GMM weights.

2.4.1 Trust-Region Updates

VIPS based algorithms exploit the lower bound from Eq. 8, which results in maximizing

$$\begin{aligned}\tilde{J}(q(o)) &= \sum_o q(o) R(o) + H(q(o)), \\ R(o) &= \mathbb{E}_{q_{\theta}(\mathbf{x}|o)} [\log \tilde{p}(\mathbf{x}) + \log \tilde{q}(o|\mathbf{x})] + H(q(\mathbf{x}|o)).\end{aligned}$$

Originally, Arenz et al. (2018) used a KL-constrained trust-region similar to the component update,

$$q^{\text{new}}(o) \propto q(o)^{\frac{\eta_w}{1+\eta_w}} \exp(\tilde{R}(o))^{\frac{1}{1+\eta_w}},\tag{11}$$

where η_w is the Lagrangian multiplier of trust region constraint, and $\tilde{R}(o)$ a Monte-Carlo estimate of the component's reward $R(o)$. Arenz et al. (2020) showed, that the weights can also be directly updated to an estimate of the optimal weights, that is,

$$q^{\text{new}}(o) \propto \exp(\tilde{R}(o)).\tag{12}$$

2.4.2 Natural Gradient Updates

Algorithms based on higher-order gradients use the natural parameters $\omega \in \mathcal{R}^{K-1}$ (K is the number of components) of the weight distribution $q(o)$ and compute the natural gradient,

$$\omega = \omega_{\text{old}} + \beta \delta$$

where each dimension δ_o of the natural gradient is given by

$$\begin{aligned}\delta_o &= \mathbb{E}_q(\mathbf{x}|o) [\log \tilde{p}(\mathbf{x}) - \log q_{\theta}(\mathbf{x})] \\ &\quad - \mathbb{E}_q(\mathbf{x}|K) [\log \tilde{p}(\mathbf{x}) - \log q_{\theta}(\mathbf{x})].\end{aligned}$$

The natural parameters relate to the weights in terms of

$$\begin{aligned}\omega_o &= \log(q(o)/q(K)), \quad \text{for } o < K, \\ q(K) &= 1 - \sum_{i=1}^{K-1} q(o).\end{aligned}\tag{13}$$

3 A Unified Perspective of NG for GMMs

The different methods presented in Section 2 both use natural gradient estimates to update the parameters of the approximation. Indeed, we will show that these methods and their variants are highly related and can be unified in a common framework. Still, they differ in many details that nevertheless may substantially affect the performance. We will now present a common formulation for these methods and discuss all the details in which they differ. By disentangling the individual design choices and their contributions to the overall performance of the algorithm, we aim to identify the most important factors for sample-efficient and accurate Gaussian mixture model variational inference. We will evaluate different combinations of design choices in Section 4 and show that a hybrid variant that combines trust-regions with higher-order natural gradients substantially outperforms any previous method for GMM based variational inference.

Table 1: Overview of Design Choices for GMM-Based VI

METHOD	NG ESTIMATE	STEP SIZE	SAMPLING	ADAPTING K	ENSURING P.D.
ARENZ ET AL. (2018)	MC, MORE	KL-BASED	FROM COMP.	HEURISTIC	BACKTRACKING
ARENZ ET AL. (2020)	MC, MORE	$\beta_w = 1$, KL-BASED	FROM COMP.	$\tilde{R}(o_{\text{NEW}})$	BACKTRACKING
LIN ET AL. (2019A)	MC, VON	FIXED, DECAYING	FROM MIXTURE	-	-
LIN ET AL. (2020)	MC, STEIN	FIXED, DECAYING	FROM MIXTURE	-	iBAYESLR

3.1 Equivalence of the NG Updates

Both, VIPS (Arenz et al., 2018; 2020) and the methods by Lin et al. (2019a; 2020), decompose the optimization problem into independent updates to the weights and components that are updated along their natural gradient.

Indeed, the weight updates (Eq. 11 and Eq. 13), and the component updates (Eq. 4 and Eq. 7) can each be transformed to each other as stated in Lemma 3.1 and Lemma 3.2. Derivations for these lemmas are provided in Appendix A, where we also proof that both decompositions of the update are equivalent.

Lemma 3.1. *Equivalence of Weight Updates. For each stepsize $\beta \in (0, 1]$ the update given by Eq. 11 can be transformed to the update given by Eq. 13, by setting $\beta = 1/(\eta_w + 1)$. Furthermore, the optimal weights given by Eq. 12 correspond to the update given by Eq. 13 with $\beta = 1$.*

Lemma 3.2. *Equivalence of Component Updates. For each stepsize $\beta \in (0, 1]$ the updates given by Eq. 4 can be transformed to the updates given by Eq. 7, by setting*

$$\beta = \frac{1}{\eta + 1}, \quad \mathbf{R} = \mathbb{E}_{h(\mathbf{x})} [\nabla_{\mathbf{x}\mathbf{x}} R(\mathbf{x})],$$

$$\mathbf{r} = \mathbb{E}_{h(\mathbf{x})} [\nabla_{\mathbf{x}\mathbf{x}} R(\mathbf{x})] \boldsymbol{\mu}_{old} - \mathbb{E}_{h(\mathbf{x})} [\nabla_{\mathbf{x}} R(\mathbf{x})].$$

Hence, these methods only differ in the way the stepsizes are chosen (for example, directly or based via trust-regions) and how the expected Hessian and the expected gradient are estimated (for example, using ordinary least-squares, or Monte-Carlo estimates using Stein’s Lemma). We will now discuss the merits of these and several other design choices, e.g., related to sample selection and component adaptation.

3.2 Natural Gradient Estimation

As we show in Appendix A, the methods by Lin et al. (2019a; 2020) and Arenz et al. (2018; 2020) use the same Monte-Carlo estimate for estimating the natural gradient with respect to the weights. For estimating the natural gradient for the Gaussian components, Arenz et al. (2018; 2020) use the zero-order method MORE (Abdolmaleki et al., 2015), which estimates the expected Hessian and the expected gradient through the parameters of a quadratic surrogate that is learned with ordinary least-squares. Lin et al. (2019a) use the second-order method VON (Khan et al., 2018) which computes the Hessian $\nabla_{\mathbf{x}\mathbf{x}} \log \tilde{p}(\mathbf{x})$ analytically for

estimating the expected Hessian with Monte-Carlo. However, computing the Hessian is often computationally too expensive, and thus, Lin et al. (2020) estimate the expected Hessian using Stein’s Lemma, which only needs access to the gradient. The first-order methods *VOGN* and *gradient magnitude*, both discussed by Khan et al. (2018), would likely be inferior as they yield a biased (and rather crude) estimate. A modification of the update in Eq. 7, the *improved Bayesian learning rule* (Lin et al., 2020) that was combined with the estimate based on Stein’s Lemma, however, is another interesting option, as it ensures the new covariance matrix is positive definite. However, this update does no longer correspond to the natural gradient.

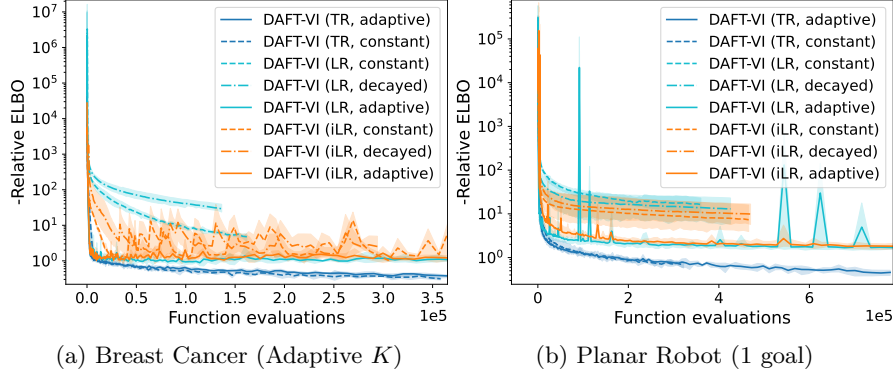


Figure 1: We compare different schemes for adapting the step size for the natural gradient update of the components. KL-constrained trust region can substantially outperform directly controlled step sizes.

3.3 Stepsize Selection

Lin et al. (2020) used fixed stepsizes in their reference implementation but used different stepsizes for weights and for the components. Khan and Lin (2017) discussed a backtracking method to adapt the stepsize while ensuring positive definiteness, but they found it slow in practice and did not test it in the GMM setting, and Khan et al. (2018) used a decaying stepsize. In contrast, Arenz et al. (2018) do not control the stepsize directly but use a trust-region method based on the Kullback-Leibler divergence to the previous weights or Gaussian component, respectively, when updating the weights and components. For obtaining the maximal stepsize that fulfills the KL constraint, they have to solve a convex optimization problem over the scalar Lagrangian multiplier, which adds computational overhead but yields more stable updates. Arenz et al. (2020) showed, that a fixed stepsize of $\beta_w = 1$ for updating the weights (which always sets the weights to their estimated optimum) works well in practice. For updating the components, they again use KL-constrained trust-regions, and adapt the bounds independently for each component, by increasing the bound if the reward of the corresponding component improved during the last update, and by decreasing the bound otherwise.

3.4 Ensuring Positive-Definiteness

Ensuring positive definite (p.d.) covariance matrices throughout the optimization can be challenging in practice. Similar to the backtracking procedure discussed by Khan and Lin (2017), Arenz et al. (2020) decrease the KL bound if an update would not produce a p.d. covariance matrix. When using fixed or decaying learning rates, sufficiently small initial learning rates may avoid the problem of non-p.d. covariance matrices (Lin et al., 2019a), but can not provide a guarantee. Hence, Lin et al. (2020) used a modified update rule that was proven to yield positive definite updates.

3.5 Sample Selection

For estimating the expected Hessian and gradient (relating to the surrogate parameters \mathbf{R} and \mathbf{r}) and the NG of the weights δ (relating to the component rewards $R(o)$) the previously discussed methods use samples that are evaluated on the target distribution. These samples are used to evaluate the Monte-Carlo estimates

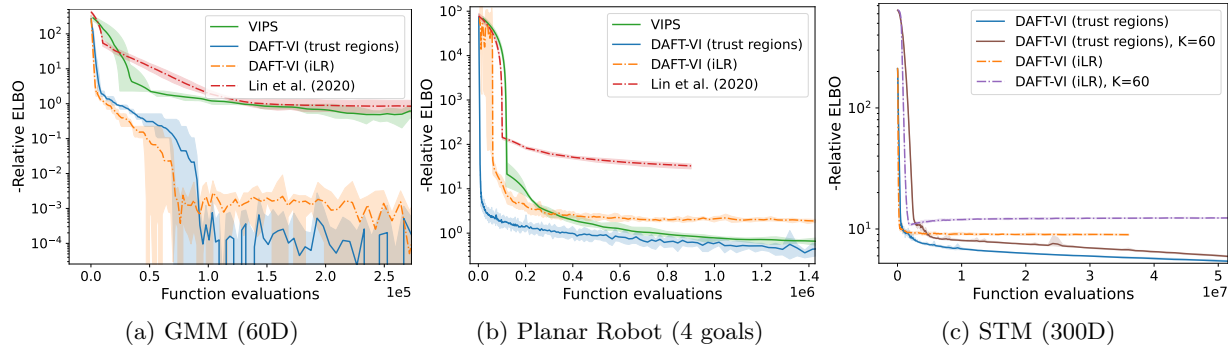


Figure 2: We evaluated the effect of adapting the number of components, which can be crucial, as seen in the GMM experiments. For the 300-dimensional mixture of Student-t a fixed number of components performed better in the long run. This is likely caused, due to the fact that we did not limit the number of components yielding a significantly large mixture (200 vs 50 components) at the end of the experiment.

of Eq. 6, to obtain data for least-squares, to estimate the component’s reward $\tilde{R}(o)$ or to estimate the natural gradient for the weights θ . The samples should be drawn from the corresponding component $q(\mathbf{x}|o)$. However, for both, the methods by Arenz et al. (2018; 2020) and the methods by Lin et al. (2019a; 2020), importance sampling (or weighted least-squares) is used in order to use samples from a different distribution. Lin et al. (2019a; 2020) draw at each iteration samples from the mixture model and use the same samples for computing each update. Arenz et al. (2018; 2020) also share samples between different components, but reuse samples from previous iterations and ensure that every component is covered by generating additional samples from each component if a given desired effective sample size is not met. As a consequence, the approach by Lin et al. (2019a; 2020) may require fewer samples per iteration and overall, at the cost of computational overhead caused by larger number of iterations and the risk of not providing meaningful updates to components with low weights.

3.6 Component Adaptation

The methods by Lin et al. (2019a; 2020) regard the number of components K as a hyperparameter, which remains constant during optimization. Arenz et al. (2018; 2020) dynamically adapt the number of components by deleting components at poor local optima that do not contribute to the approximation, and by adding new components in promising regions. Arenz et al. (2018) used a heuristic that takes into account the unnormalized target density (stored together with previous samples in a buffer) and the current model density at these locations, to decide at which sample location the new component should be initialized. Arenz et al. (2020) refined this procedure by deriving a similar score as an estimate of the initial reward $\tilde{R}(o_{\text{new}})$ for the new component. They showed that adapting the number of components can be crucial for obtaining an accurate approximation of challenging multimodal target distributions as the learned GMM is less reliant on the initialization and can actively explore regions based on previous function evaluations.

3.7 Algorithm Overview

The different design choices for the discussed methods are shown in Table 1. Algorithm 1 (Appendix B) shows pseudocode for generalizing the different methods to illustrate the different steps that are performed at each iteration. Here we describe the algorithm in terms of Eq. 4 and Eq. 13, however, Eq. 7 and Eq. 11 could be used likewise. Please note that \mathbf{R}_o and \mathbf{r}_o can be computed from $\nabla_{\mathbf{x}\mathbf{x}}R_o(\mathbf{x})$ and $\nabla_{\mathbf{x}}R_o(\mathbf{x})(\mathbf{x})$ and δ can be computed from $R(o)$.

4 Experiments

Based on our analysis in Section 3, we are particularly interested in comparing (1) trust-region based stepsize selection against direct stepsize control, (2) the effect of adapting the number of components, and (3) the

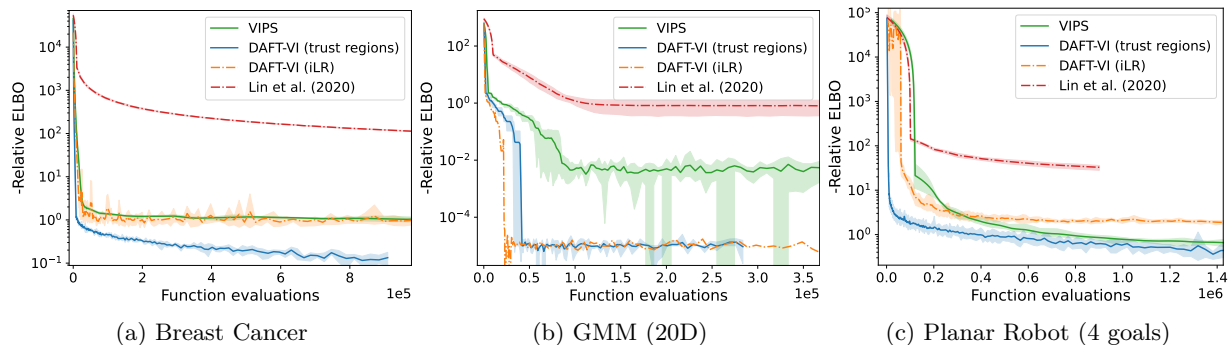


Figure 3: Our proposed methods (blue) and its variant (orange) clearly outperform previous methods (Lin et al., 2020; Arenz et al., 2020).

performance of zero-order based MORE against the first-order based Stein’s Lemma for approximating expected Hessians and gradients. If not stated otherwise, we use first-order estimates (Stein’s Lemma, Lin et al., 2020) and adaptive number of components and adaptive trust regions. We refer to this set of design choices as *double adaptive, first-order estimates, and trust regions for VI* (DAFT-VI). However, we will evaluate the effect of these design choices independently.

We have based our implementations on the reference implementations provided by Arenz et al. (2020) and Lin et al. (2020). However, the reference implementations used C++ and Matlab, respectively, which made it difficult for us to extend them or to run them on a cluster. Hence, we ported each implementation to Python (Tensorflow) and verified that the performances were comparable. Most of our experiments are based on our port of the code by Arenz et al. (2020) because it includes features such as adapting the number of components and trust region optimization. We performed our experiments on test problems from both Lin et al. (2020) and Arenz et al. (2020), namely we use two logistic regression experiments (on the *breast cancer* and *German credit* data set, Lichman, 2013), the planar robot experiments, and GMM experiments (where we increased the number of dimensions to up to 100) from Arenz et al. (2020) and the 20-dimensional and 300-dimensional mixture of Student-T experiments from Lin et al. (2020). Please refer to Appendix C for a description of the test problems.

4.1 Trust-Regions vs Learning Rates

In our first set of experiments we want to compare the performance of KL-constrained trust-regions against directly controlling the stepsize. We tested eight different settings for stepsize selection: $(TR, constant)$ and $(TR, adaptive)$ (aka DAFT-VI) find for each component update the largest step that stays below a given KL-constraint, where the latter approach adapts the bound as proposed by Arenz et al. (2020). For optimizing the step, we implemented a simple line search, because we found it more robust than L-BFGS-B (Byrd et al., 1995), which was used by Arenz et al. (2018; 2020). The remaining six settings were all related to directly controlling the stepsize, where we tested fixed stepsizes, decaying stepsize and adaptive stepsize with the natural gradient step (Eq.7), which we denote $(LR, constant)$, $(LR, decayed)$, and $(LR, adaptive)$, and with the alternate update proposed by (Lin et al., 2020) for ensuring positive definiteness, which we denote $(iLR, constant)$, $(iLR, decayed)$, and $(iLR, adaptive)$. For decaying learning rates, we used the procedure described by Khan et al. (2018), and for the adaptive stepsize, we used the same procedure as Arenz et al. (2020) used for updating the KL constraints, namely, we multiplied the stepsize by a factor larger than 1, if the performance of a component improved during the last step (based on the Monte-Carlo estimate $\tilde{R}(o)$) and with factor smaller than 1 if it degraded. Please refer to Appendix D for details on the hyperparameters and their optimization for all our experiments. Figure 1 shows the performance of the different choices on the *breast cancer* and *Planar robot* experiment. In both experiments, the KL-constrained trust-regions outperform direct learning rate control, even when choosing a constant trust region, by a large margin.

4.2 Adapting the Number of Components

We evaluated the impact of adapting the number of components based on the procedure described by Arenz et al. (2020). Here we compared adaptive GMMs with non-adaptive GMMs, each with trust region updates and with learning rate-based updates, where we used the best settings from the previous experiment (*TR, adaptive*) and (*iLR, adaptive*). Figure 2 shows that the adaptive variants outperformed the variants with fixed number of components.

4.3 Zero-Order vs First-Order NG Estimate

Our proposed algorithm, DAFT-VI, differs from VIPS (Arenz et al., 2020) mainly by using Stein’s Lemma for estimating the surrogate parameters \mathbf{R}_o and \mathbf{r}_o . In our main experiment, we evaluate how this difference affects the performance of the algorithm, by comparing it with our Python port of the reference code of VIPS (Arenz et al., 2020). We also compare with our port of the reference implementation provided by Lin et al. (2020), which, however, could not achieve competing performance. We further compare with our variant (*iLR, adaptive*), in order to further investigate the performance of trust-region based optimization, compared to direct learning rate control, which is significantly more common in the field of variational inference. Figure 3 shows the learning curves for these methods with tuned hyperparameters on *breast cancer*, the 20-dimensional *GMM*, and the *planar robot* experiment with four goals. The remaining results are shown in Appendix E. DAFT-VI clearly outperforms both VIPS and the method by Lin et al. (2020) and overall performed also better than our variant (*iLR, adaptive*).

5 Related Work

In addition to the aforementioned methods, several other methods have explored natural gradients and trust-regions for variational inference. For mean-field approximations, Hoffman et al. (2013) propose an efficient method for estimating the natural gradient from mini-batches, and Theis and Hoffman (2015) proposed a related KL-constrained trust-region method. Regier et al. (2017) proposed a second-order method for Gaussian variational inference based on Euclidean trust-regions. Khan et al. (2015) introduced a KL-based proximal point method for conjugate models and related it to natural gradient descent. For non-conjugate models, they proposed local linearizations. Khan et al. (2016) extended this approach to other divergences and stochastic gradients. Salimbeni et al. (2018) compute the natural gradient based on the Jacobian of the parameters of the Gaussian and its expectation parameters. The Jacobian can be computed using forward-mode differentiation, or by using reverse-mode differentiation twice. For GMM-based variational inference, Miller et al. (2017) and Guo et al. (2016) proposed a boosting method, which, however, requires unreasonably large mixture models, because components that have been added at previous iterations do not longer receive updates. Recently, Lin et al. (2021) investigated natural gradient GMM-based variational inference, with structured covariance matrix, which may be important for scaling these methods to higher dimensions.

6 Conclusion

We investigated recent natural gradient based methods for GMM based variational inference and showed that their updates to weights and components are actually equivalent. Still, these methods differ in several algorithmic choices that substantially affect the performance in terms of sample efficiency and the quality of the learned approximation. We evaluated several of these choices. Based on our experiments, KL-constrained trust regions—even when applied on top of higher-order natural gradients—seem to outperform directly controlled learning rates, and dynamically adapting the number of components has clear advantages compared to optimizing GMMs with fixed number of components. Based on these insights, we proposed a novel method that combines fast first-order based estimates of the natural gradients with adaptive KL-constrained trust regions and adaptive number of components, setting a new standard for GMM based variational inference.

References

- Ivan Kobyzev, Simon Prince, and Marcus Brubaker. Normalizing flows: An introduction and review of current methods. *IEEE Transactions on Pattern Analysis and Machine Intelligence*, 2020.
- Marco Ewerton, Oleg Arenz, and Jan Peters. Assisted teleoperation in changing environments with a mixture of virtual guides. *Advanced Robotics*, 34(18):1157–1170, 2020. doi: 10.1080/01691864.2020.1785326.
- Emmanuel Pignat, Teguh Lembono, and Sylvain Calinon. Variational inference with mixture model approximation for applications in robotics. In *2020 IEEE International Conference on Robotics and Automation (ICRA)*, pages 3395–3401. IEEE, 2020.
- O. Arenz, M. Zhong, and G. Neumann. Efficient gradient-free variational inference using policy search. In *International Conference on Machine Learning (ICML)*, 2018.
- Wu Lin, Mohammad Emtiyaz Khan, and Mark Schmidt. Fast and simple natural-gradient variational inference with mixture of exponential-family approximations. In *International Conference on Machine Learning*, pages 3992–4002. PMLR, 2019a.
- Wu Lin, Mark Schmidt, and Mohammad Emtiyaz Khan. Handling the positive-definite constraint in the Bayesian learning rule. In Hal Daumé III and Aarti Singh, editors, *Proceedings of the 37th International Conference on Machine Learning*, volume 119 of *Proceedings of Machine Learning Research*, pages 6116–6126. PMLR, 13–18 Jul 2020.
- Oleg Arenz, Mingjun Zhong, and Gerhard Neumann. Trust-region variational inference with gaussian mixture models. *Journal of Machine Learning Research*, 21(163):1–60, 2020. URL <http://jmlr.org/papers/v21/19-524.html>.
- A. Abdolmaleki, R. Lioutikov, N. Lua, L. Paulo Reis, J. Peters, and G. Neumann. Model-based relative entropy stochastic search. In *Advances in Neural Information Processing Systems (NeurIPS)*, pages 153–154, 2015.
- Wu Lin, Mohammad Emtiyaz Khan, and Mark Schmidt. Stein’s lemma for the reparameterization trick with exponential family mixtures. *arXiv preprint arXiv:1910.13398*, 2019b.
- Solomon Kullback and Richard A Leibler. On information and sufficiency. *The annals of mathematical statistics*, 22(1):79–86, 1951.
- Jan Peters, Katharina Mulling, and Yasemin Altun. Relative entropy policy search. In *Twenty-Fourth AAAI Conference on Artificial Intelligence*, 2010.
- John Schulman, Sergey Levine, Pieter Abbeel, Michael Jordan, and Philipp Moritz. Trust region policy optimization. In *International conference on machine learning*, pages 1889–1897. PMLR, 2015.
- Fabian Otto, Philipp Becker, Vien Anh Ngo, Hanna Carolin Maria Ziesche, and Gerhard Neumann. Differentiable trust region layers for deep reinforcement learning. In *International Conference on Learning Representations*, 2021. URL <https://openreview.net/forum?id=qYZD-A01Vn>.
- J. Pajarinen, H.L. Thai, R. Akrou, J. Peters, and G. Neumann. Compatible natural gradient policy search. (8):1443–1466, 2019.
- Richard S Sutton, David McAllester, Satinder Singh, and Yishay Mansour. Policy gradient methods for reinforcement learning with function approximation. In S. Solla, T. Leen, and K. Müller, editors, *Advances in Neural Information Processing Systems*, volume 12. MIT Press, 2000. URL <https://proceedings.neurips.cc/paper/1999/file/464d828b85b0bed98e80ade0a5c43b0f-Paper.pdf>.
- Mohammad Emtiyaz Khan and Didrik Nielsen. Fast yet simple natural-gradient descent for variational inference in complex models. In *2018 International Symposium on Information Theory and Its Applications (ISITA)*, pages 31–35. IEEE, 2018.

-
- Mohammad Khan and Wu Lin. Conjugate-computation variational inference: Converting variational inference in non-conjugate models to inferences in conjugate models. In *Artificial Intelligence and Statistics*, pages 878–887. PMLR, 2017.
- Mohammad Khan, Didrik Nielsen, Voot Tangkaratt, Wu Lin, Yarin Gal, and Akash Srivastava. Fast and scalable Bayesian deep learning by weight-perturbation in Adam. In Jennifer Dy and Andreas Krause, editors, *Proceedings of the 35th International Conference on Machine Learning*, volume 80 of *Proceedings of Machine Learning Research*, pages 2611–2620. PMLR, 10–15 Jul 2018.
- Manfred Opper and Cédric Archambeau. The variational gaussian approximation revisited. *Neural computation*, 21(3):786–792, 2009.
- Charles M Stein. Estimation of the mean of a multivariate normal distribution. *The annals of Statistics*, pages 1135–1151, 1981.
- M. Lichman. UCI machine learning repository, 2013. URL <http://archive.ics.uci.edu/ml>.
- R.H. Byrd, P. Lu, J. Nocedal, and C. Zhu. A limited memory algorithm for bound constrained optimization. *SIAM Journal on Scientific Computing*, 16(5):1190–1208, 1995.
- Matthew D. Hoffman, David M. Blei, Chong Wang, and John Paisley. Stochastic variational inference. *Journal of Machine Learning Research*, 14(4):1303–1347, 2013. URL <http://jmlr.org/papers/v14/hoffman13a.html>.
- L. Theis and M. Hoffman. A trust-region method for stochastic variational inference with applications to streaming data. In *International Conference on Machine Learning (ICML)*, pages 2503–2511. PMLR, 2015.
- Jeffrey Regier, Michael I Jordan, and Jon McAuliffe. Fast black-box variational inference through stochastic trust-region optimization. In *Proceedings of the 31st International Conference on Neural Information Processing Systems*, pages 2399–2408, 2017.
- Mohammad Emtiyaz Khan, Pierre Baqué, François Fleuret, and Pascal Fua. Kullback-leibler proximal variational inference. In *Proceedings of the international conference on Neural Information Processing Systems*, number CONF, 2015.
- Mohammad Emtiyaz Khan, Reza Babanezhad, Wu Lin, Mark Schmidt, and Masashi Sugiyama. Faster stochastic variational inference using proximal-gradient methods with general divergence functions. In *Proceedings of the Thirty-Second Conference on Uncertainty in Artificial Intelligence*, pages 319–328, 2016.
- Hugh Salimbeni, Stefanos Eleftheriadis, and James Hensman. Natural gradients in practice: Non-conjugate variational inference in gaussian process models. In *International Conference on Artificial Intelligence and Statistics*, pages 689–697. PMLR, 2018.
- A. C. Miller, N. J. Foti, A. D’Amour, and R. P. Adams. Variational boosting: Iteratively refining posterior approximations. In *International Conference on Machine Learning (ICML)*, 2017.
- F. Guo, X. Wang, K. Fan, T. Broderick, and D. B. Dunson. Boosting variational inference. *arXiv:1611.05559v2 [stat.ML]*, 2016.
- Wu Lin, Frank Nielsen, Khan Mohammad Emtiyaz, and Mark Schmidt. Tractable structured natural-gradient descent using local parameterizations. In Marina Meila and Tong Zhang, editors, *Proceedings of the 38th International Conference on Machine Learning*, volume 139 of *Proceedings of Machine Learning Research*, pages 6680–6691. PMLR, 18–24 Jul 2021. URL <https://proceedings.mlr.press/v139/lin21e.html>.

A Equivalence of the Discussed NG Updates

We will now prove Lemma 3.1 and 3.2, thereby showing that VIPS (Arenz et al., 2020) and the methods by Lin et al. (2019a; 2020) use the same update equation for weights, means and covariance matrices.

A.1 Weight Update of Lin et al. (2019a; 2020)

Lin et al. (2020) formulate the weight update in the natural parameter space,

$$\boldsymbol{\omega} = \boldsymbol{\omega}_{\text{old}} + \beta \boldsymbol{\delta} \quad (14)$$

where each dimension $\boldsymbol{\delta}_o$ of the natural gradient is given by

$$\begin{aligned} \boldsymbol{\delta}_o = & \mathbb{E}_q(\mathbf{x}|o) [\log \tilde{p}(\mathbf{x}) - \log q_{\boldsymbol{\theta}}(\mathbf{x})] \\ & - \mathbb{E}_q(\mathbf{x}|K) [\log \tilde{p}(\mathbf{x}) - \log q_{\boldsymbol{\theta}}(\mathbf{x})]. \end{aligned}$$

Defining

$$\hat{R}(o) = \mathbb{E}_q(\mathbf{x}|o) [\log \tilde{p}(\mathbf{x}) - \log q_{\boldsymbol{\theta}}(\mathbf{x})],$$

the i -th index of the natural parameters is given by

$$\boldsymbol{\omega}_i = \boldsymbol{\omega}_{\text{old},i} + \beta \hat{R}(o) - \beta \hat{R}(K).$$

The new weight of component $o < K$ is given by

$$\begin{aligned} q(o; \boldsymbol{\omega}) &= \frac{\exp(\boldsymbol{\omega}_o)}{\left[\sum_{k=1}^{K-1} \exp \boldsymbol{\omega}_k \right] + 1} \\ &= \frac{\exp(\boldsymbol{\omega}_{\text{old},o} + \beta \hat{R}(o) - \beta \hat{R}(K))}{\left[\sum_{k=1}^{K-1} \exp(\boldsymbol{\omega}_{\text{old},k} + \beta \hat{R}(k) - \beta \hat{R}(K)) \right] + 1} \\ &= \frac{\frac{q(o)_{\text{old}}}{q(K)_{\text{old}}} \exp(\beta \hat{R}(o))}{\left[\sum_{k=1}^{K-1} \frac{q(k)_{\text{old}}}{q(K)_{\text{old}}} \exp(\beta \hat{R}(k)) \right] + \exp \beta \hat{R}(K)} \\ &= \frac{q(o)_{\text{old}} \exp(\beta \hat{R}(o))}{\left[\sum_{k=1}^{K-1} q(k)_{\text{old}} \exp(\beta \hat{R}(k)) \right] + q(K)_{\text{old}} \exp(\beta \hat{R}(K))}. \end{aligned}$$

Hence, for all components (including K), we have

$$q(o) \propto q(o)_{\text{old}} \exp(\beta \hat{R}(o)). \quad (15)$$

A.2 Weight Update (VIPS)

We start by expressing the component's reward $R(o)$ in terms of $\hat{R}(o)$, namely,

$$\begin{aligned} R(o) &= \mathbb{E}_{q_{\boldsymbol{\theta}}(\mathbf{x}|o)} \left[\log \tilde{p}(\mathbf{x}) + \log \tilde{q}(o|\mathbf{x}) \right] + H(q(\mathbf{x}|o)) \\ &= \mathbb{E}_{q_{\boldsymbol{\theta}}(\mathbf{x}|o)} \left[\log \tilde{p}(\mathbf{x}) + \log q(o|\mathbf{x}) - \log q(\mathbf{x}|o) \right] \\ &= \mathbb{E}_{q_{\boldsymbol{\theta}}(\mathbf{x}|o)} \left[\log \tilde{p}(\mathbf{x}) + \log q(o) - \log q(\mathbf{x}) \right] = \hat{R}(o) + \log q(o), \end{aligned}$$

where we exploited that the auxiliary distribution is chosen according to the true responsibilities, $\tilde{q}(o|x) = q(o|x)$.

Expressing the weight update of VIPS (Equation 11) in terms of $\hat{R}(o)$,

$$\begin{aligned} q(o) &\propto \left[q_{\text{old}}(o)^{\frac{\eta_w}{1+\eta_w}} \exp(R(o))^{\frac{1}{1+\eta_w}} \right. \\ &= q_{\text{old}}(o)^{\frac{\eta_w}{1+\eta_w}} \exp\left(\hat{R}(o) + \log q_{\text{old}}(o)\right)^{\frac{1}{1+\eta_w}} \\ &= q_{\text{old}}(o) \exp\left(\frac{1}{1+\eta_w} \hat{R}(o)\right) \left. \right], \end{aligned}$$

we can see that it exactly matches the update in Equation 15 for $\beta = \frac{1}{1+\eta_w}$. \square

A.3 Equivalence of the Component Updates

We restate the VIPS update (Equation 4),

$$\begin{aligned} \Sigma &= \left(\frac{\eta}{\eta+1} \Sigma_{\text{old}}^{-1} - \frac{1}{\eta+1} \mathbf{R} \right)^{-1}, \\ \mu &= \Sigma \left(\frac{\eta}{\eta+1} \Sigma_{\text{old}}^{-1} \mu_{\text{old}} + \frac{1}{\eta+1} \mathbf{r} \right), \end{aligned}$$

and the update by Lin et al. (2019a) (Eq. 7),

$$\begin{aligned} \Sigma &= \left((1-\beta) \Sigma_{\text{old}}^{-1} - \beta \mathbb{E}_{h(\mathbf{x})} [\nabla_{\mathbf{x}\mathbf{x}} \log \tilde{p}(\mathbf{x})] \right)^{-1} \\ \mu &= \Sigma \left((1-\beta) \Sigma_{\text{old}}^{-1} \mu_{\text{old}} - \beta \mathbb{E}_{h(\mathbf{x})} [\nabla_{\mathbf{x}} \log \tilde{p}(\mathbf{x})] \right. \\ &\quad \left. - \beta \mathbb{E}_{h(\mathbf{x})} [\nabla_{\mathbf{x}\mathbf{x}} \log \tilde{p}(\mathbf{x})] \mu_{\text{old}} \right), \end{aligned}$$

for your convenience. Comparing both updates, we can see that they are equivalent, for

$$\beta = \frac{1}{\eta+1},$$

$$\mathbf{R}_o = \mathbb{E}_{h(\mathbf{x})} [\nabla_{\mathbf{x}\mathbf{x}} \log \tilde{p}(\mathbf{x})], \quad (16)$$

$$\mathbf{r}_o = \mathbb{E}_{h(\mathbf{x})} [\nabla_{\mathbf{x}\mathbf{x}} \log \tilde{p}(\mathbf{x})] \mu_{\text{old}} - \mathbb{E}_{h(\mathbf{x})} [\nabla_{\mathbf{x}} \log \tilde{p}(\mathbf{x})]. \quad (17)$$

So far, we only showed that both updates share the same form. We still need to show, that using MORE (Abdolmaleki et al., 2015) on the VIPS lower bound 8,

$$\begin{aligned} \tilde{J}(\tilde{q}, \theta) &= \sum_o q(o) \left[\int_{\mathbf{x}} q_{\theta}(\mathbf{x}|o) \left(\log \tilde{p}(\mathbf{x}) + \log \tilde{q}(o|\mathbf{x}) \right) d\mathbf{x} \right. \\ &\quad \left. + H(q_{\theta}(\mathbf{x}|o)) \right] + H(q_{\theta}(o)) \\ &= J(\theta) - \int_{\mathbf{x}} q_{\theta}(\mathbf{x}) \text{KL}(q(o|\mathbf{x}) || \tilde{q}(o|\mathbf{x})) d\mathbf{x}, \end{aligned}$$

yields the same unbiased estimate of the expected Hessian and gradient (when transforming the reward parameters according to Eq. 16 and Eq.17), as estimating the expected Hessian and gradient on the objective (Eq. 10) derived by Lin et al. (2019a),

$$\begin{aligned} \tilde{J}_{q(\mathbf{x}|o)} &= \int_{\mathbf{x}} q(\mathbf{x}|o) \log \frac{\tilde{p}(\mathbf{x})}{q(\mathbf{x})} d\mathbf{x} \\ &= \mathbb{E}_{q(\mathbf{x}|o)} [f(\mathbf{x})] \text{ with } f(\mathbf{x}) = \log \tilde{p}(\mathbf{x}) - \log q(\mathbf{x}). \end{aligned}$$

However, we note that when computing the component update, the lower VIPS lower bound 8 can be written as an expectation of the same function $f(x) = \log \tilde{p}(\mathbf{x}) - \log q(\mathbf{x})$ as in Eq. 10, since the auxiliary distribution \tilde{q} is update to the current model q_θ . The gradients and Hessians $\nabla_{\mathbf{x}} f(\mathbf{x})$ and $\nabla_{\mathbf{xx}} f(\mathbf{x})$ will coincide, and so will the estimate (for example using Stein’s Lemma). \square

B Pseudocode for the Unified NG GMM Update

Algorithm 1 Natural Gradient GMM Variational Inference

```

for  $i = 1$  to MAXITER do
  Draw / reuse samples
  Estimate  $\delta$  (Monte-Carlo)
  Estimate  $\mathbf{R}_o, \mathbf{r}_o$  (e.g. MORE, VON, Stein’s Lemma)
  Select stepsizes  $\beta_w, \beta_o$  (trust-region, constant, decay, adaptive)
   $\eta_o = \frac{1}{\beta_o} - 1$ 
  Update components (Eq. 4)
  Update weights (Eq. 13)
  Adapt Components (Optional)
end for

```

C Test Problems

We performed the experiments on target distributions taken from related work. For details, please refer to the corresponding work. The *breast cancer*, *German credit*, *planar robot* and *GMM* experiment were used by Arenz et al. (2020) and the Student-T experiments were used by Lin et al. (2020).

- In the *breast cancer* (*BC*) and *German credit* (*GC*) we aim to approximate the posterior distribution of a logistic regression problem. The dimensions are 25 and 31, respectively. The data sets can be obtained from the UCI Machine Learning Repository (Lichman, 2013) and contain 1000 and 569 data points.
- In the planar robot experiment, we aim to sample joint configurations of a 10-link *planar robot* (all links have the same length) and aim to reach either a single, or one of four goal positions (*Planar1* and *Planar4* resp.). The target distribution is Gaussian in the endeffector configuration space (but non-Gaussian in the joint configuration space). A zero-mean Gaussian prior on the joint angles is additionally used to prevent non-smooth configuration.
- In the *GMM* experiment we aim to approximate an unknown Gaussian mixture model with 10 components and varying number of dimensions. Arenz et al. (2020) only considered 60 dimensions, but we increased the dimensionality to up to 100. The mean is sampled uniformly in the range $[-50, 50]$ and the covariance matrices $\Sigma = \mathbf{A}^\top \mathbf{A} + I$ are created by randomly sampling the elements of the square matrix \mathbf{A} .
- The mixture of Student-T experiment (*STM*), is similar to the *GMM* experiment but uses Student-T components instead of Gaussians. We exactly follow Lin et al. (2020) by considering a 20-dimensional mixture with 10 components with mean uniformly sampled in $[-20, 20]$, and a 300-dimensional mixture with 20 components sampled in $[-25, 25]$.

C.1 Offset for ELBO plots

For a better readability and an increase of the resolution in the plots we subtracted constant offsets from the ELBOs. The offsets are given in 2.

Table 2: Subtracted ELBO offsets per experiment

Breast Cancer	German Credit	Planar 1	Planar 4	Breast Cancer (GVA)	STM300
78.08	585.0943	12.43	11.86	78.779	11.16

Table 3: Selected number of (reused, desired) samples per component and update step. Lin et al. (2020) do not reuse old samples.

Experiment	DAFT(trust region)	DAFT (iLR)	Lin et al. (2020)	VIPS
GMM20	(200, 100)	(100, 50)	100	(800, 400)
GMM40	(400, 200)	(100, 50)	100	(1600, 800)
GMM60	(400, 200)	(200, 100)	100	(2400, 1200)
GMM80	(400, 200)	(200, 100)	100	N/A
GMM100	((400, 200))	(100, 50)	100	N/A
Planar1	(100, 50)	(200, 100)	100	(400, 200)
Planar4	(40, 20)	(100, 50)	1000	(400, 200)
STM20	(900, 450)	(400, 200)	100	(800, 400)
STM300	(800, 400)	(900, 450)	N/A	N/A
BC	(400, 200)	(800, 400)	100	(500, 1000)
GC	(400, 200)	(200, 100)	100	(620, 1240)

D Hyperparameters

For the DAFT-VI algorithm, we automatically adapt the KL bound based on the scheme proposed by Arenz et al. (2020). The same adaptation can be implemented for the stepsize in the improved learning rate update. Here we use a smaller initial learning rate of 5×10^{-5} to obtain more stable updates. The method by Lin et al. (2020) incorporates separate learning rates for the component and the weight update. A fixed component step size of 1×10^{-5} is used in our implementation. We noticed that fixing the weights uniformly produced better results than updating them with a separate learning rate. This was also done in some experiments in Lin et al. (2020). It remains to select the number of samples per update step. We follow the scheme proposed by Arenz et al. (2020) for drawing new samples. Namely, we specify the number of reused samples N_{reused} and the number of desired samples N_{desired} . At every iteration we select the $N_{\text{components}} \times N_{\text{reuse}}$ newest samples for importance sampling. We then compute for every component the number of effective samples $n_{\text{eff}}(o)$ based on the importance weights, and draw $n_{\text{new}} = n_{\text{desired}} - \lfloor n_{\text{eff}}(o) \rfloor$ new samples. In contrast to that, Lin et al. (2020) do not reuse old samples but choose a fixed amount of new data points from the mixture model per update step.

We conducted a preliminary evaluation with a single seed for each algorithm (except for VIPS, where we used the parameters from Arenz et al. (2020)) and test problem to select the N_{desired} and N_{reused} (the new samples per iteration for Lin et al. (2020) respectively). The chosen hyperparameters per experiment are given in Table 3.

E Additional Experiments

The additional experiments are shown in Figure 4. Here, we show our main experiment on all test problems, and also compare the different methods in a Gaussian VI setting on the *breast cancer* experiment (where DAFT-VI does not adapt the number of components). In all experiments, DAFT-VI and its variant DAFT-VI (iLR) significantly outperform the previous methods by Arenz et al. (2020) and Lin et al. (2020).

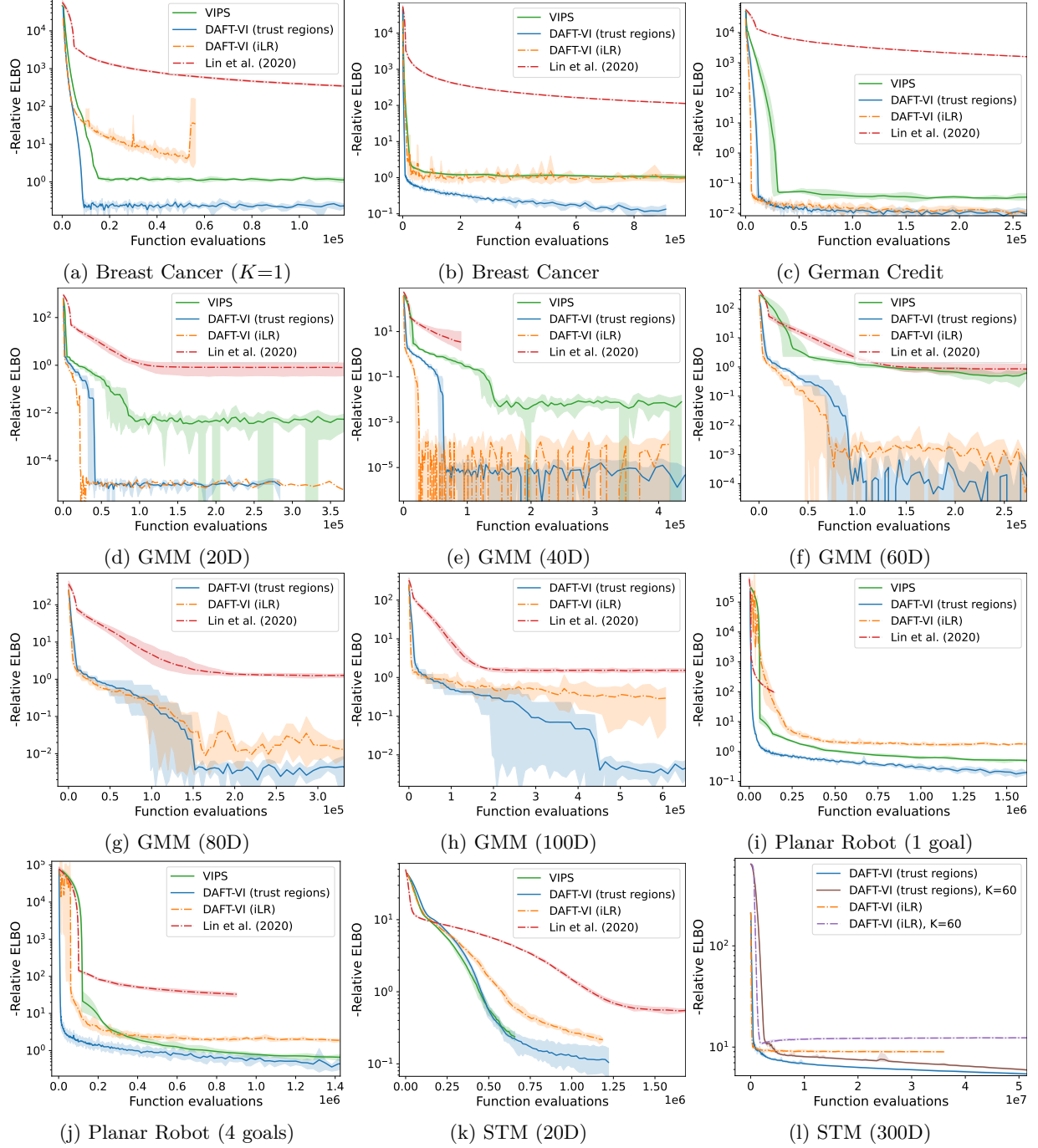


Figure 4: We compare DAFT-VI with prior methods on several test problems.